



Phytochemical Analysis of Phragmites Australis Aerial Parts Extract By LC–ESI–MS and its Silver Nanoparticles as Well as their Biological Activities

Ahmed M. Al-Sayed ¹, Reham E. Shafek ^{*1}, Nabila H. Shafik ¹, Helana N. Michael ¹,
Ali A. Ali ², Farg Abdelhai ².

¹ Chemistry of Tanning Materials and Leather Technology Department, National Research Centre, Dokki, Cairo, Egypt.

² Chemistry Department, Faculty of Science, Al-Azhar University, Nasr City 11884, Cairo, Egypt



CrossMark

In Loving Memory of Late Professor Doctor ””Mohamed Refaat Hussein Mahran””

Abstract

The chemical components, cytotoxic effect, antioxidant and antimicrobial activities of Phragmites australis aerial parts 70% aqueous ethanolic extract were examined. Its chromatographic techniques were employed to identify polar and non-polar components in the extract. Chromatographic and chemical investigations of its extract revealed the existence of 2 phenolic acids, 2 C- glycoside flavones, 4 flavones, 10 flavonoids and 4 flavanone which were isolated for the first time from its aerial parts. Their structures were deduced via detailed spectroscopic interpretation. All 22 isolated compounds were tentatively identified using LC–ESI–MS. The ethanolic extract was used for preparation silver nano particles producing them less than 20 nm. P. australis extract and its AgNPs were tested for antioxidant activity which showed that AgNPs extract reduced antioxidant activity by 33% as compared to P. australis extract (69%) while that of vitamin C (81%). The two extracts were tested in vitro against human cancer cells A431, PC3, HCT116, and the normal cell line BJ1 (normal skin fibroblast) using doxorubicin as the reference medication were revealed that all of the examined samples had a modest to no cytotoxic effect on the cancer cells tested. Finally, the antimicrobial results for both extracts showed a significant influence with some fluctuation depending on the strain type.

1. Introduction

The Poaceae family of monocotyledonous flowering plants was once known as the Gramineae family. Undoubtedly the most abundant and significant family among Earth's flora, the Poaceae constitute the single most important source of food on the planet. They can be found growing on every continent, in freshwater and marine environments, deserts, and all elevations below the highest ones. Grass-dominated plant groups make for around 24% of all vegetation on Earth. Its members, which number over 12,000 species and 780 genera [1], are significant to human agriculture, the economy, and the environment. They are also distinguished by the presence of flavonoid and flavone C glycoside chemicals [2]. This family's common reed, Phragmites australis (P. australis), is found in semi-aquatic environments and is the source of numerous chemical.

China traditionally uses P. australis leaves as a flavoring in food preparation. An evaluation was

carried on the antiviral and anti-inflammatory properties of a water-soluble extract obtained from P. australis leaves. and found that P. australis leaf may be a promising herb for the creation of new antiviral and anti-inflammatory drugs [3, 4]. It is used to treat various diseases in humans and animals in traditional medicine [5, 6]. Aquatic extracts from P. australis rhizomes showed antioxidant and hepatoprotective qualities. Additionally, leaf extract has been shown to have antioxidant and anti-melanogenesis properties [7, 8]. Its water-soluble extracts have also been shown to have antiviral properties. In Chinese Traditional medicine, P. australis rhizomes have long been used in traditional lung diseases. Additionally, it was stated that hepatitis could be cured with P. australis rhizome [9]. Due to the isolation of numerous active ingredients, including terpenoids, flavonoids, coumarins, acetylenes, caffeoylquinic acids and sterols. it also has significant medicinal value.

In addition to preparing its silver nanoparticle extract (AgNPs) using AgNO₃, the current study

*Corresponding author e-mail: rehamshafek1971@gmail.com

Receive Date: 25 December 2023, Revise Date: 10 January 2024, Accept Date: 05 February 2024

DOI: 0.21608/ejchem.2024.258168.9073

©2024 National Information and Documentation Center (NIDOC)

aims to investigate the phytochemical studies and biological activities of aerial parts of *Phragmites australis* 70% aqueous ethanolic extract (*P. australis* ext.). To do this, it will isolate and chemically characterize its polyphenolic constituents using various chromatographic techniques such as paper and column chromatography and chemical analysis e.g. complete and controlled acid hydrolysis beside the enzymatic hydrolysis, where 22 phenolic and flavonoid compounds were discovered for the first time (Table 1). The compounds were analyzed using ^1H NMR, ^{13}C NMR, and LC-ESI-MS. The cytotoxicity of four human carcinoma cell lines (A431, PC3, HCT116, and BJ1) as well as the two extracts of *P. australis* and its AgNPs were assessed in comparison to DPPH. Apart from examining their effects on gram-positive (*Bacillus cereus*, *Staphylococcus aureus*), gram-negative (*Escherichia coli*, *Pseudomonas aeruginosa*), and pathogenic yeast.

2. Experimental

2.1. Materials and Methods

Plant material:

Aerial parts of *P. australis* were collected from Mit gammer (Dakalia governorate, Egypt), in September 2019 and authenticated by Dr. Mona M. Marzouk, Department of Phytochemical and Plant Systematics, NRC. A voucher specimen (sn. M3314) was deposited in the Herbarium of NRC (CAIRC, Cairo, Egypt)

Chemicals and instruments:

NMR experiments were recorded on a Jeol EX-500 spectrophotometer: 500 MHz (^1H NMR), 125 MHz (^{13}C NMR), UV spectrophotometer (Shimadzu UV-240), LC-QTOF-HR-MS/MS Triple TOF 5600+, column chromatography (CC) Polyamide 6S (Riedel-De-Haen AG, SeelzeHaen AG, SeelzeHanver, Germany), and Sephadex LH-20 (Pharmazia) using EtOH/H₂O as eluent. Paper chromatography (PC) for preparative (PPC) on Whatman No. 1 and 3 MM papers, utilizing solvent systems: 1) H₂O, 2) 15% HOAc, 3) 6% HOAc, 4) BAW (n-BuOH-HOAc-H₂O 6:1:2). To detect the aglycones and sugar moieties, complete acid hydrolysis (2 N HCl, 2 h, 100°C) and mild acid hydrolysis (0.1 N HCl, 1 hour, 100°C) were performed, followed by paper co-chromatography with authentic samples..

Extraction and isolation

The dried aerial parts of *P. australis* were extracted thoroughly with 70% aqueous ethanol and dried under vacuum before being filtered and defatted with petroleum ether (40-60°C). The residue was slurred with water, mixed with a tiny amount of polyamide, and then exposed to a polyamide CC,

beginning with water as the eluent and gradually reducing the polarity by increasing the concentration of ethanol up to 100%. Using H₂O, 15% AcOH, and BAW as eluents, ten fractions were produced and categorized based on their PC features. The fractions were tested using both FeCl₃ and the Shinoda's reagent, which revealed the existence of substances with high phenolic and flavonoid content. For the separation and purification of flavonoid chemicals, PPC was used. The paper descending techniques were employed in all glass chromatography tanks. The chromatograms were air-dried and checked before being exposed to ammonia vapours to see if the colours of the spots changed. Finally, 10 fractions were collected, dried, and purified again on Sephadex LH-20 columns to yield the isolated chemicals. R_f-values, colour reactions, chemical studies complete and mild acid hydrolysis besides enzymatic hydrolysis, physical investigations (UV and ^1H NMR, ^{13}C NMR), and LC-ESI-MS were used to identify these isolated compounds (Table 1).

Chemical data for some isolated compounds

Quercetin-3-O- β -xyloside (1): Yellow amorphous powder. UV/Vis λ_{max} (nm) (MeOH) 355 (6.65), 257 (6.74) nm; (NaOAc) 371.5 (6.58), 272.5 (6.76) nm; (NaOAc/ H₃BO₃) 375.5 (6.70), 261 (6.83) nm; (AlCl₃) 430 (6.68), 273 (6.82) nm; (AlCl₃/HCl) 400 (6.60), 270 (6.78) nm; ^1H -NMR (500 MHz, DMSO-*d*₆) Aglycone moiety: δ (ppm) δ : 7.6 (1H, H-2'), 7.57 (1H, d, J=2.1 Hz, H-6'), 6.84 (1H, s, H-5'), 6.39 (1H, d, J=1.8 Hz, H-8), 6.16 (1H, d, J=2.1 Hz, H-6), 5.17 (1H, d, J=7.2 Hz, H-1''), 3.78 (1H, dd, J=11.4; 5.0 Hz, H-5''), 3.46-3.54 (2H, m, H-3'', H-4''), 3.39 (1H, m, H-2''), 3.1 (1H, dd, J=11.5; 9.5 Hz, H-5''); ^{13}C NMR (CD₃OD; 75 MHz) δ 179.4 (C, C-4), 166.0 (C, C-7), 163.1 (C, C-5), 158.5 (C, C-2), 158.5 (C, C-9), 149.8 (C, C-3'), 146.1 (C, C-4'), 135.4 (C, C-3), 123.3 (CH, C-6'), 123.0 (C, C-1'), 117.2 (CH, C-5'), 115.9 (CH, C-2'), 105.6 (C, C-10), 104.5 (CH, C-1''), 99.8 (CH, C-6), 94.7 (CH, C-8), 77.5 (CH, C-3''), 75.3 (CH, C-2''), 71.0 (CH, C-4''), 67.2 (CH₂, C-5'').

Hesperetin -7-O-neohesperidoside (2): ^1H -NMR (500 MHz, DMSO-*d*₆) δ H: 11.91 (1H, s, 5-OH), 9.14 (1H, s, 3'-OH), 6.95 (1H, s, H-5'), 6.93 (1H, s, H-2'), 6.88 (1H, dd, J=10.0, 1.5 Hz, H-6'), 6.11 (1H, s, H-6), 6.08 (1H, s, H-8), 5.52 (1H, dd, J=4.0, 2.0 Hz, H-2), 5.33 (1H, s, OH), 5.12 (1H, d, J=2.0 Hz, H-1'), 5.11 (1H, s, H-1'''), 4.74 (1H, s, OH), 4.60 (1H, s, OH), 4.52 (1H, OH), 3.77 (3H, s, 4'-OCH₃), 3.67 (3H, m), 3.45 (4H, m), 3.35 (1H, m, H-3 α), 3.20 (1H, m), 2.76 (1H, dd, J=4.0, 2.0 Hz, H-3 β), 1.14 (3H, d, J=6.5 Hz, H-6'''); ^{13}C -NMR (DMSO-*d*₆) δ : 78.58 (C-2), 42.36 (C-3), 197.16 (C-4), 162.78 (C-5), 96.48 (C-6), 165.04 (C-7), 95.33 (C-8), 162.78 (C-9), 117.97, 103.20 (C-10), 131.10 (C-1'), 112.22 (C-2'), 146.70 (C-3'), 148.17 (C-4'), 114.31 (C-

5'), 100.57(C-1''), 76.26(C-2''), 77.33(C-3''), 69.78(C-4''), 77.09(C-5''), 97.61(C-1'''), 70.56(C-2'''), 70.65(C-3'''), 72.01(C-4'''), 68.46(C-5'''), 18.22(C-6'''), 55.88(4'-OCH₃), 60.61(C-6'').

Apigenin 8-C-β-D-glucopyranosyl: ¹H-NMR (500 MHz, DMSO-d₆) δH:6.49 (1H, s, H-8), 6.54 (1H, s, H-3), 6.96 (2H, d, J = 8.6 Hz, H-3', 5'), 7.81(2H, d, J = 8.6 Hz, H-2', 6'), 3.52 (1H, m, H-5''), 3.54 (1H, m, H-3''), 3.57 (1H, m, H-4''), 3.74 (1H, dd, J = 12.3, 5.5 Hz, H-6a''), 3.77 (1H, dd, J = 12.3, 2.0 Hz, H-6b''), 4.14 (1H, t, J = 9.0 Hz, H-2''), 4.81 (1H, d, J = 9.9 Hz, H-1''),. ¹³C-NMR (DMSO-d₆) δ (ppm): 61.3 (C-6''), 70.6 (C-4''), 72.5 (C-2''), 74.5 (C-1''), 79.7 (C-3''), 81.6 (C-5''), 95.1(C-8), 103.7 (C-3), 104.3 (C-10), 108.7 (C-6), 116.3 (C-3', 5'), 122.5 (C-1'), 129.0 (C-2',6'), 157.4 (C-9), 160.3 (C-5), 162.0 (C4'), 164.5 (C-7), 165.4 (C-2), 183.6 (C-4).

LC–ESI–MS analysis

Materials and methods

Equipment and conditions

Fragmentation analyses were performed using (Triple TOF 5600+). The mobile phases consisted of DI-Water containing 0.1% FA (formic acid), ammonium format buffer pH=8 containing 1% methanol and 100 % acetonitrile, in-Line filter discs Pre column (0.5 μm x 3.0 mm, Phenomenex), X bridge C18 column (3.5 μm, 2.1x50 mm, waters) and the column temperature was maintained at 40°C, flow rate 0.3 ml/min and the scan type (Information Dependent Acquisition (IDA)).

Sample preparation

P. australis were defatted and desalted by CHCl₃ and, respectively, by warming under reflux conditions. The mobile phase working solution (MP-WS) was prepared from DI-Water-Methanol-Acetonitrile (50: 25: 25 v/v). Add 1 ml of MP-WS to 50 mg weighted sample, vortex for 2 min followed by ultra-sonication for 10 min, and centrifuge for 5 min at 10000 rpm. An amount of 20 μl stock (50/1000 μl) was diluted with 1000 μl reconstitution solvent. Finally, the injected concentration was 1μg/μl. Inject 25 μl from the total extract on positive mode and 25 μl MP-WS as a blank sample.

Data processing

Master View was used for feature peaks extraction from the total ion chromatogram (TIC) based on features that should have Signal-to-Noise greater than 5 (Non-targeted analysis). Features intensities of the sample-to-blank should be greater than 5. Marker View was used for feature annotation and removing isotopic peaks. Master View was used again to identify peaks based on their fragments using Built-in database and online database; RESPECT and MONA (Mass Bank of North America).

Green synthesis of silver nanoparticles

Because of its cheap cost-effectiveness, convenience of availability, and therapeutic characteristics, the biosynthesis of AgNPs with *P. australis* ext. was chosen. *P. australis* ext. was prepared in the same manner as previously reported. The extracted substance was dried, powdered, and stored.

In a 250-ml Erlenmeyer flask, an aqueous solution of 1 mM silver nitrate (AgNO₃) was produced and utilized to synthesize AgNPs. In brief, three different con. of *P. australis* extract were produced, added to an aqueous solution of 1 mM silver nitrate, and incubated overnight at room temperature in the dark. The color change from colorless to colloidal brownish yellow confirmed the full reduction of AgNO₃ to Ag⁺ ions. The colloidal liquid was then appropriately packed and kept for future use. A spectrophotometric study confirmed the production of AgNPs [10].

DPPH assay

With some slight adjustments, the antioxidant capacity of *P. australis* extract and Ag NPs. of *P. australis* was tested using a DPPH technique defined by employing the free radical 2,2-diphenyl-picrylhydrazyl (DPPH). After 30 minutes of incubation at room temperature, aliquots (0.1 mL) of diluted extracts in methanol were added to 1 mL of DPPH solution, and the absorbance of the DPPH solution was measured at 517 nm. To compare the antioxidant capacity of *P. australis* extracts, appropriate blanks (methanol) and standards (Trolox solution in methanol) were utilized. All measurements were taken three times. Using the equation [11], the radical-scavenging activity (RSA) was determined as a percentage of DPPH discoloration.

$$\% \text{ RSA} = (A_{\text{blank}} - A_{\text{sample}} / A_{\text{blank}}) \times 100 \quad (\text{Equation 1})$$

Cell culture

A431 skin cancer and prostate cancer (PC3) were maintained in DMEM medium, and HCT-116 colorectal carcinoma, BJ1 normal skin fibroblast were maintained in RPMI. All media were supplemented with 10% foetal bovine serum and incubated at 37 °C in 5% CO₂ and 95% humidity. Cells were subcultured using trypsin versene 0.15%. All cell lines were purchased from Vacsera (Giza, Egypt).

Cytotoxic effect on human cell lines.

Cell viability was assessed by the mitochondrial-dependent reduction of yellow MTT (3-(4,5-dimethylthiazol-2-yl)-2,5-diphenyl tetrazolium bromide) to purple formazan [12]. Procedure: All the following procedures were done in a sterile area using a Laminar flow cabinet biosafety class II level (Baker, SG403INT, Sanford,

ME, USA). Cells were suspended in DMEM-F12 medium [(for A431 (skin cancer), PC3 (prostate cell line), HCT116 (colon cell line)] beside one normal cell line (BJ1), 1% antibiotic-antimycotic mixture (10,000U/ml Potassium Penicillin, 10,000µg/ml Streptomycin Sulphate and 25µg/ml Amphotericin B) and 1% L-glutamine at 37 °C under 5% CO₂.

Cells were batch cultured for 10 days, then seeded at a concentration of 10×10^3 cells/well in fresh complete growth medium in 96-well microtiter plastic plates at 37 °C for 24 h under 5% CO₂ using a water-jacketed Carbon dioxide incubator (Sheldon, TC2323, Cornelius, OR, USA). Media was aspirated, fresh medium (without serum) was added and cells were incubated either alone (negative control) or with different concentrations of sample to give a final concentration of (100-50-25-12.5-6.25-3.125-0.78 and 1.56 µg/ml). After 48 h of incubation, the medium was aspirated, 40µl MTT salt (2.5µg/ml) was added to each well and incubated for further four hours at 37°C under 5% CO₂. To stop the reaction and dissolve the formed crystals, 200µL of 10% Sodium dodecyl sulphate (SDS) in deionized water was added to each well and incubated overnight at 37°C. A positive control composed of 100µg/ml was used as a known cytotoxic natural agent that gives 100% lethality under the same conditions [12]. The absorbance was then measured using a microplate multi-well reader (Bio-Rad Laboratories Inc., model 3350, Hercules, California, USA) at 595nm and a reference wavelength of 620nm. A statistical significance was tested between samples and negative control (cells with the vehicle) using an independent t-test by SPSS 11 program. DMSO is the vehicle used for the dissolution of plant extracts and its final concentration in the cells was less than 0.2%. The percentage of change in viability was calculated according to the formula (Equation 2):

$$\left(\frac{\text{Reading of extract}}{\text{Reading of negative control}} - 1 \right) \times 100 \quad (\text{Equation 2})$$

A probit analysis was carried out for IC₅₀ and IC₉₀ determination using SPSS 11 program. In the present study, the degree of selectivity of the synthetic compounds is expressed as SI=IC₅₀ of the pure compound in a normal cell line/IC₅₀ of the same pure compound in a cancer cell line, where IC₅₀ is the concentration required to kill 50% of the cell population.

Antimicrobial Activity

Qualitative evaluations were carried out in nutrient broth according to [13-14]. The inoculation of pathogenic microorganisms used in this study were Gramme-positive bacteria (*Bacillus cereus* & *Staphylococcus aureus*), Gramme-negative bacteria (*Escherichia coli* & *Pseudomonas aeruginosa*), and pathogenic yeast (*Candida albicans*), was prepared from fresh overnight broth

cultures using nutrient broth medium that were incubated at 37°C [15]. The inoculum size of this pathogenic strain was prepared and adjusted to approximately 0.5 McFarland standard (1.5×10^8 CFU/ml) [15], and 25.0 µL inoculum size of each microorganism strain was separately inoculated into each plate containing 20.0 ml of the sterile nutrient agar medium (NA). The samples were applied After the media cooled and solidified on a 0.9 cm well of that inoculated agar plates which were prepared previously by using a 1.0 cm cork borer applying the Well Diffusion Method, in this method each well was filled with 100.0 µl of each sample separately [15].

3. Results and Discussion

Phenolics investigation of polyphenolic compounds

LC-QTOF-HR-MS/MS was used to determine the polyphenolic 2RY metabolites in *P. australis* 70% aqueous ethanolic extract. The limit of detection for each peak of chemicals was calculated using the RT, full MS spectra, and MS². Literature and reference compound spectra were compared to identify fragmentation patterns in the negative mode as shown in Fig [1]. 22 components were investigated in *P. australis* ethanolic extract (Table 1), as phenolic acids: chlorogenic acid (1), and rosmarinic acid (2). Flavonoids: Luteolin-3', 7-di-*O*-glucoside (3), Kaempferol-7-neohesperidoside (4), Isorhamnetin-3-*O*-rutinoside (5), Hesperetin-7-*O*-neohesperidoside (6), Isosakuranetin-7-*O*-neohesperidoside (7), Eriodictyol-7-*O*-neohesperidoside (8), Kaempferol-3-*O*-glucouronouide (9), Baicalein-7-*O*-glucuronide (10), Luteolin-7-*O*-glucoside (11), Luteolin-8-C-glucoside (12), Apigenin 8-C-glucoside (13), Kaempferol-3-*O*-(6'-*p*-coumaroyl)-glucoside (14), Luteolin-6-C-glucoside (15), Quercetin-3-*O*-xyloside (16), Isorhamnetin-3-*O*-glucoside (17), Kaempferol-3-*O*-rhamnoside (18), Quercitrin (19), Myricetin (20), Apigenin (21), Hesperetin (22).

Phenolic acids are a type of secondary metabolite (SM) with a number of intriguing metabolic processes. They often create the pseudomolecular ion [M- H]⁻, which corresponds to a deprotonated molecule, and the distinctive fragmentation [M - H-44], which is associated to CO₂ loss from the carboxylic acid group. Two free phenolic acids, chlorogenic and rosmarinic, were initially found in this study according to their molecular ion peaks at m/z 353.0860 and 359.1039.

Six flavonoid diglycosides were discovered in *P. australis* Comparable to (peaks 3, 4, 5, 6, 7, and 8). Luteolin-3', 7-di-*O*-glucoside, Kaempferol-7-neohesperidoside, Isorhamnetin-3-*O*-rutinoside, Hesperetin-7-*O*-neohesperidoside, Isosakuranetin-7-

O-neohesperidoside,
neohesperidoside.

Peak 3 contained a molecular ion peak at *m/z* 609.1482 and particular fragment ions at *m/z* 327.04819, 357.02969, 447.08875 [M-H-162] - and 489.0929 [M-H-120]- which di glucose sugar units are losed, so it recognized as luteolin-3', 7-di-*O*-glucoside.

Peak 4 had a molecular ion peak at *m/z* 593.1441 and separate fragment ions at *m/z* 341.0665, 429.08008, 447.10104 [M-H-146]- and 285.0398 [M-H-(146+162)]- as a result of rhamnose and glucose unit losses, respectively.

Peak 5 displayed a signal for a molecular ion at *m/z* 623.1610 and characteristic fragment ions at *m/z* 473.0970, 477.04791[M-H-146]-, 315.0477 [M-H-(146+162)]-, 255.04561, 257. 0092 due to the loss of rhamnose and glucose units, respectively hence peak 5 was recognized as isorhamnetin-3-*O*-rutinoside.

Peak 6: deprotonated molecule at *m/z* 609.565 [M - H] - with chemical formula C₂₈H₃₄O₁₅ which was identified as Hesperetin-7-*O*-neohesperidoside with a molecular fragment ions at *m/z* 447.0835[M-H-146]-, 285.0547 [M-H-(146+162)]- as a result of rhamnose and glucose unit losses, respectively.

peak 7 was identified as isosakuranetin-7-*O*-neohesperidoside, with a molecular ion peak at *m/z* 593.1251 and distinct fragment ions at *m/z* 447.0835[M-H-146]-, 285.0547 [M-H-(146+162)]- as a result of rhamnose and glucose unit losses, respectively.

Peak 9: according to the ESI-MS-MS spectrum peak 9 was identified as Kaempferol-3-Glucuronide based on its molecular ion peak at *m/z* 461.0484 and intense product ions at *m/z* 285.2497, 309.04062.

Peak 10: The ESI-MS-MS spectrum for Compound 10 is the same as that for baicalein-7-*O*-glucuronide based on MS/MS analysis (The peak at *m/z* 445.1304 in the ESI-MS spectrum can be explained as the flavonoid [M -H]-. The peak at *m/z* 269 can be described as the flavonoid's aglycone part [M -H-glucuronide], hence compound 10 is defined as baicalein-7-*O*-glucuronide.

Using LC-Q-TOF-HR-MS/MS analysis nine flavonoid monoglycosides were detected in *p. Australis* ext. corresponding to Luteolin-7-*O*-glucoside, Luteolin 8-C-glucoside, apigenin 8-C-glucoside, Kaempferol-3-*O*-(6-*p*-coumaroyl)-glucoside, Luteolin-6-C-glucoside, Quercetin-3-*O*-xyloside, Isorhamnetin-3-*O*-glucoside, Kaempferol-3-*O*- rhamnoside and Quercetin -3-*O*- rhamnoside (Quercitrin) (peaks 11-19).

Peak (12, 15) was tentatively identified them as luteolin 8-glucoside and luteolin 6-glucoside, respectively. Based on their intensive fragment at *m/z* 327.123 [M-H-120]-, 357.06851 [M-H-90]- and varied retention duration, two luteolin derivatives at the same molecular ion peak *m/z* 447 were

Eriodictyol-7-*O*-

established. They were generated from luteolin aglycone.

Peak 13: one derivatives of apigenin at molecular ion peak *m/z* 431 were tentatively established based on their intensive fragment at *m/z* 311[M-H-120]-, 341.06851 [M-H-90]- which indicated that they were derived from apigenin aglycone. They were tentatively identified as apigenin 8-glucoside.

Peak 16: The aglycone quercetin has been verified by the distinctive characteristics fragment ion at *m/z* 301, and the neutral ion loss of 132 amu in both compounds suggested the loss of a xyloside unit and was subsequently identified as quercetin-3-*O*-xyloside.

Peak 17 was determined to be Isorhamnetin-3-*O*-glucoside due to the loss of the glucose moiety and the distinctive deprotonated fragment at *m/z* 315.05316[M-H -162] - and product ions at *m/z* 179.002 and 151.9352.

Peak 18: The fragmentation pattern and the characteristic fragment at *m/z* 285.5290 confirmed kaempferol as aglycone. and distinct fragment ions at *m/z* 431.1797 [M-H-146]- as a result loose of rhamnose unite.

Peak 19: MS profiling of compound 19 produced adeprotonated molecular ion at *m/z* 447.2515 and fragment ions at 301. 2011 [M-H-164] , 401.1257, 279.2339. 269.0305. The aglycone quercetin was identified by this characteristic ion fragments. The compound was identified as quercitrin.

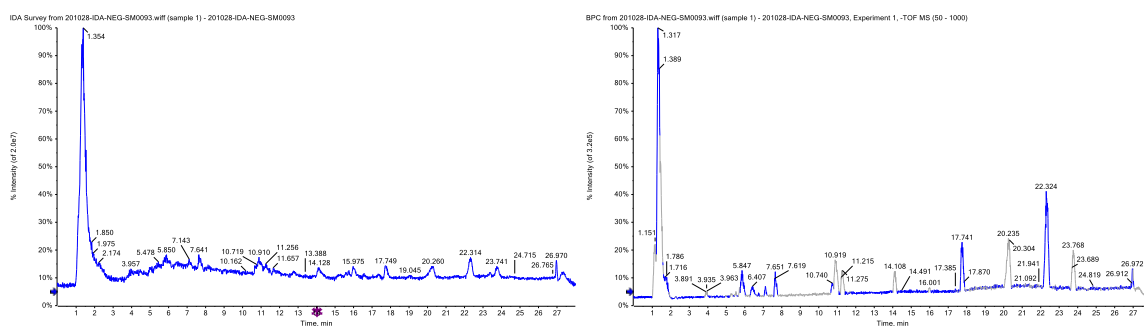
Based on MS/MS analysis, Peaks (20, 21 and 22) showing the fragment ions 286.0417, 283.0509, 255.2368, 174.0286 for hesperetin and the fragment ions 151.00, 153.10, 225.00, 117. 200, 227.0350 for apigenin, a [M-H]-ions at *m/z* 317.1002 and the fragment ions at *m/z* 287.0823, 180.9735, 112.9857 for myricetin.

SM0136: Negative-MODE – TIC and BPC

Green synthesis of silver nanoparticles

UV-visible spectra

P. australis extract was employed to make Ag nanoparticles. For the synthesis of Ag nanoparticles, three distinct con were employed. The appearance of brownish-yellow color is thought to be confirmation that Ag nanoparticles have developed. Due to the mutual oscillation of electrons in metal nanoparticles in resonance with light waves, Ag nanoparticles have free electrons, which produce a surface plasmon resonance (SPR) absorption band. The emergence of the peaks demonstrates the surface plasmon resonance properties of silver nanoparticles[29]. Figure 2 depicts the UV-vis spectra of Ag nanoparticles generated when three distinct strains of *P. australis* were added to a 10 mL solution of 10-3 M AgNO₃. In its as-prepared state, the SPR band generates absorption in the visible area of the samples between 485 and 495 nm.

Fig. [1]: Negative-MODE – TIC and BPC of *P. australis* extract.**Table [1]: LC-ESI-MS analysis of phenolic compounds of *P. australis* extract**

Peak No	RT m	Identified Compound	Classes	[M-H] ⁻¹	Err or (ppm)	Molecular Formula	Fragment Ions	Ref
1	1.795	Chlorogenic acid	Phenolic acid	353.0860	-0.6	C ₁₆ H ₁₈ O ₉	284.09557, 191.0571, 179.0356, 173.0454	16
2	2.146	Rosmarinic acid	Phenolic acid	359.1039	1.1	C ₁₈ H ₁₆ O ₈	179.0567, 161.0468, 143.0345	17
3	5.213	Luteolin-3', 7-di-O-glucoside	Flavonoid-3', 7-di-O-glycosides	609.1482	-0.2	C ₂₇ H ₃₀ O ₁₆	447.0871, 285.10711	18
4	5.713	Kaempferol-7-neohesperidoside	Flavonoid-7-O-glycosides	593.1441	3.5	C ₂₇ H ₃₀ O ₁₅	285.0398, 447.10104, 341.0665, 311.0549	19
5	6.219	Isorhamnetin-3-O-rutinoside	Flavonoid-3-O-glycosides	623.1610	-1.8	C ₂₈ H ₃₂ O ₁₆	577.2075, 315.0477	17
6	7.919	Hesperetin-7-O-neohesperidoside	Flavonoid-7-O-glycosides	609.565	0.2	C ₂₈ H ₃₄ O ₁₅	591.1439, 301.0697	20
7	8.325	Isosakuranetin-7-O-neohesperidoside	Flavonoid-7-O-glycosides	593.1251	4.4	C ₂₈ H ₃₄ O ₁₄	285.0547, 447.5009, 431.08901	21
8	8.460	Eriodictyol-7-O-neohesperidoside	Flavonoid-7-O-glycosides	595.2087	-0.3	C ₂₇ H ₃₂ O ₁₅	577.2061, 533.1834, 287.0205	22
9	4.210	Kaempferol-3-O-glucuronide	Flavonoid-3-O-glucuronides	461.0484	-7.2	C ₂₁ H ₁₈ O ₁₂	341.1045[M-120], 252.8917	23
10	4.325	Baicalein-7-O-glucuronide	Flavonoid-7-O-glucuronides	445.1304	-0.9	C ₂₁ H ₁₈ O ₁₁	425., 325., 269.5012, 219.0638, 175.0739, 161.0259, 121.0329	24
11	5.365	Luteolin-7-O-glucoside	Flavonoid-7-O-glycosides	447.1331	-0.8	C ₂₁ H ₂₀ O ₁₁	285.006	25
12	5.766	Luteolin-8-C-glucoside	Flavonoid- C-glucosid	447.0881	7	C ₁₂ H ₂₀ O ₁₁	327.0492[M-H-120], 357.0618[M-H-90], 299.0593	26
13	6.250	Apigenin 8-C-glucoside	Flavones	431.0979	-1.9	C ₂₁ H ₂₀ O ₁₀	311.0568[M-H-120]-, 283.0595, 341.0523, 271.001, 226.9647	27
14	6.787	Kaempferol-3-O-(6-p-coumaroyl)-glucoside	Flavonoid 3-O-coumaroyl glycosides	593.1506	4.8	C ₃₀ H ₂₆ O ₁₃	285.0426, 447.9113	28
15	7.323	Luteolin-6-C-glucoside	Flavonoid- C-glucosid	447.0889	-0.3	C ₂₁ H ₂₀ O ₁₁	357.0616, 285.0462	29
16	8.481	Quercetin-3-O-xyloside	Flavonoid- O-glucosid	433.1436	17.7	C ₂₀ H ₁₈ O ₁₁	301.1010	30
17	9.707	Isorhamnetin-3-O-glucoside	Flavonoid-3-O-glycosides	477.1174	0.3	C ₂₂ H ₂₂ O ₁₂	462.1010, 432.8943, 315.07919, 286.4936, 228.9319	31
18	10.465	Kaempferol-3-O-alpha-L-rhamnoside	Flavonoid-3-O-glycosides	431.1797	-2.1	C ₂₁ H ₁₉ O ₁₀	285.5290	32
19	10.564	Quercitrin	Flavonoid- O-glucosid	447.2515	-0.5	C ₂₁ H ₂₀ O ₁₁	401.1257, 301. 2011, 279.2339, 269.0305	33
20	10.635	Myricetin	Flavonoid- O-glucosid	317.1002	-0.5	C ₁₅ H ₁₀ O ₈	287.0823, 180.9735, 112.9857	34
21	10.705	Apigenin	Flavones	269.0438	7.9	C ₂₁ H ₂₀ O ₁₀	151.00, 153.10, 225.00, 117. 200, 227.0350	35
22	10.805	Hesperetin	4'-O-methylated flavonoids	301.694	-1.3	C ₁₆ H ₁₄ O ₆	286.0417, 283.0509, 255.2368, 174.0286	36

The inclusion of *P. australis* extract gradually increases the intensity of the SPR band. More Ag⁺ ions are being converted into Ag nanoparticles as the SPR band becomes stronger. As a result, as concentration increases, several functional groups are capable of reducing and chelating Ag nanoparticles. As demonstrated in Figure 2, the optimal concentration of *P. australis* extract for nanoparticle stability is 300.

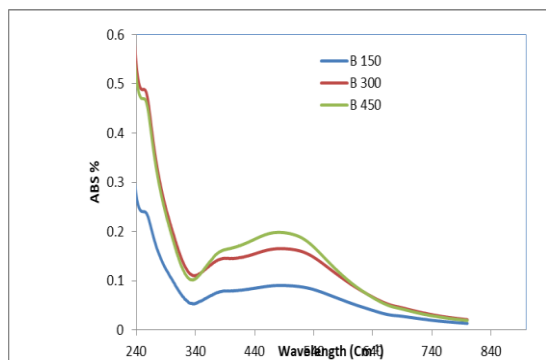


Fig. 2- UV-visible spectra for synthesized silver nanoparticles using aerial parts ethanol extract of *P. australis*

The UV-Visible spectra showed a conspicuous broad peak at 455 nm, and the broadening of the peak revealed that the particles were polydispersed (Fig. 2). AgNPs exhibit a UV-Visible absorption maximum in the 400–500 nm range due to surface plasmon resonance [10].

HRTEM analysis

Transmission electron microscopy (TEM) image of silver nanoparticles using *P. australis* ext. at room temperature. The TEM images in Fig. 3 show that the Ag NP forms have a spherical shape and particle sizes ranging from 8 to 30 nm at different magnifications [29].

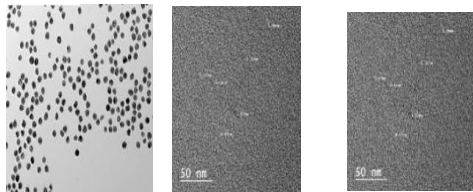


Fig. 3 TEM micrographs of synthesized AgNPs using the *phragmites australis* ethanolic extract of *phragmites australis* leaves at (a) room temperature

The TEM picture of Ag NPs generated from *P. australis* leaf extract results in spherical particles due to functional groups capable of reducing and chelating Ag nanoparticles, as shown in the accompanying figure. According to TEM pictures at various magnifications, the particle sizes of the generated Ag NPs range from 8 to 30 nm. [30].

FT-IR spectroscopy

Fourier Transform Infrared Spectroscopy (FTIR) ethanolic extract

Information about organic compounds on the surface of the nanoparticle was disclosed by the infrared spectra. FTIR spectrum analysis was used to determine the likely biomolecules of *P. australis* aerial parts extract that were responsible for reducing and capping the bio reduced silver nanoparticles. To examine the chemical makeup of different organic compounds, Fourier transform infrared spectroscopy, or FTIR, is employed. Metal nanoparticles were prepared using *P. australis* leaf extract, and FTIR analysis was performed to identify the likely biomolecules involved in capping and efficient stabilization [31]. This study's FTIR analysis shows different bond strains at different peaks: The N-H stretch is 3440.94; the C=C is 1947.75; the C=O is 1125.56; the single aldehyde is 2846.28; and the C-H is 2649.19. The OH and aldehydic C-H stretching peaks are shown in Figure 4 at 3447 cm⁻¹, 2927 cm⁻¹, and 2856 cm⁻¹, respectively. The weaker band at 1616 cm⁻¹ is amide I, which results from protein carbonyl stretch. The amine's C-N stretching vibration corresponds to the peak at 1113 cm⁻¹. The non-conjugated C=C stretching is represented by the peak near 1746 cm⁻¹. The C=CH₂ peak at 835 cm⁻¹, as well as the CH out of plane bending vibrations peaks at 679 cm⁻¹ and 657.96 cm⁻¹, are substituted ethylene systems (CH=CH (cis). [32]. The FTIR spectra of silver nanoparticles revealed prominent peaks at 2,908, 1,608, and 1,376 cm⁻¹. The stretching vibration of the (NH) C=O group caused a conspicuous and strong absorption band at 1,631 cm⁻¹ in the spectra. Stretching vibrations of C-C and C-N were allocated to band 1,383; a sharp peak at 2,908 cm⁻¹ was given to C-H and C-H (methoxy compounds) stretching vibrations, respectively [33].

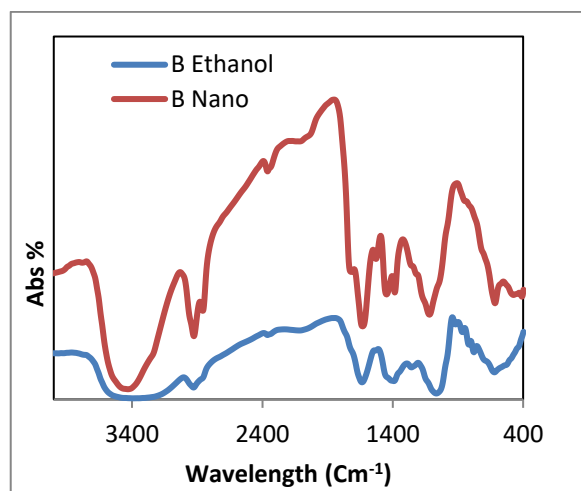


Fig. 4 (FTIR) of *P. australis* ext. and Ag NBs of *P. australis*

B nano = Ag NBs of *P. australis* B = *P. australis* ext.

Cytotoxic activity

P. australis ext. and *P. australis* Ag NBs ext. were tested in vitro against human cancer cells A431, PC3, HCT116, and the normal cell line BJ1 (normal skin fibroblast) using doxorubicin as the reference medication. This study found the medication dose that reduces survival by half (IC_{50}). Table 2 shows the results for the two extracts, while Table 3 shows the results for the standard (Doxorubicin Reference Standard) and the results revealed that all of the examined samples had a modest to no cytotoxic effect on the cancer cells tested, with the nano extract improving the cytotoxic effect.

Because of the rising interest in discovering a treatment for tumors with minimal side effects, antitumor medicines derived from plant components are becoming more popular up to this date; the anticancer activity of *P. australis* has only been briefly discussed in papers [34]. As a result, the cytotoxicity of *P. australis* and its Ag NPs against skin cancer cell lines A431 and HCT-116, as well as normal skin fibroblast BJ-1, was investigated. First, extracts at a concentration of 100 g/ml were applied to cultures of several cell lines. The cytotoxic effect was looked into (Table 2).

The nano extract which exhibited a strong cytotoxic against A-431, PC3 and HCT116 (98.7% and 95.3%, 99.4 respectively), unfortunately the strong effect of Ag nanoparticles on BJ1 normal skin cell line 100 % that is unsuitable for normal cell line [34].

Table 2: Cytotoxicity of *P. australis* ext. and Ag NBs ext. of *P. australis* at 100 µg/ml on three human tumor cell lines and one normal cell line.

Sample Code	Cytotoxic activity % at 100 (µg/ml) against the human tumor cell line(s)			
	A431	PC3	HCT116	BJ1
B	19.9	20.1	18.8	2.1
B nano	98.7	95.3	99.4	100

B nano = Ag NBs of *P. australis* B = *P. australis* ext. For most active which showed high cytotoxic effect of tested cancer cell line more than 75 % dose responses study at different concentration of (100-50-25-12.5-6.25-3.125-0.78 and 1.56 µg/ml) to calculate IC_{50} value
Positive control: Adrinamycin (doxorubicin) [Mw = 579.99]

Table 3: IC_{50} (µg/ml) against A431 , PC3, HCT116 and BJ1

Sample Code	IC_{50} value (µg/ml)			
	A431	PC3	HCT116	BJ1
B nano	30.8	28.7	24.6	20.7
Doxorubicin	24.9	26.1	37.6	13.5

A431 (skin cancer), PC3 (prostate cell line), BJ1 (normal skin fibroblast), HCT116 (colon cell line)

DPPH activity

The stable free radical (DPPH) was used to assess the radical scavenging activity of *P. australis* whole extract and *P. australis* AgNPs extract (Table 4). *P. australis* ext. inhibits chelating ability 69% more than AgNPs (33%). It is particularly significant in cancer prevention due to its antioxidant effect. The antioxidant activity of *P. australis* ext. and AgNPs ext. was investigated. When *P. australis* ext. was converted to AgNPs, antioxidant activity was lowered by 33% when compared to *P. australis* ext. (69 %) Furthermore, as indicated in the image, *P. australis* ext. has antioxidant activity comparable to vitamin C (81%) as shown in (Fig 5). This could be due to the release of flavonoids and phenolics during the nanoparticle formation process, as these compounds are responsible for plant antioxidant activity [35, 36]. This could be due to the presence of phenolic and flavonoid compounds.

Table 4: Free radical scavenging activity of samples using DPPH assay at concentration of 100 (µg/ml)

Extracts	Chelating power [Inhibition % (B)]
Total Extract of <i>P. australis</i>	69 %
AgNPs ext. of <i>P. australis</i>	33 %
Vitamin C	81 %

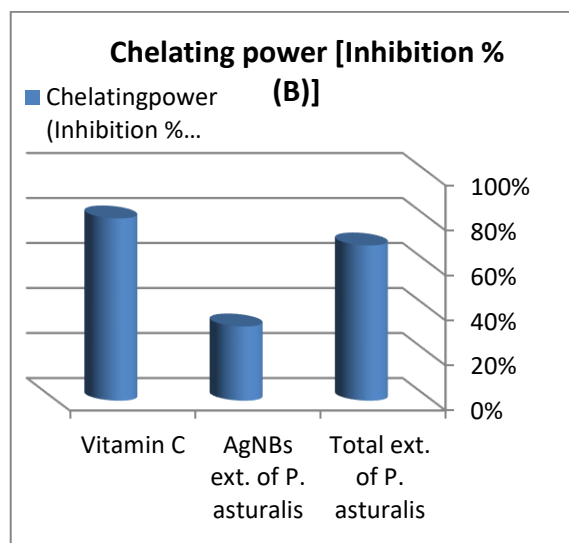


Fig [5] Free radical scavenging activity of *P. australis* and AgNPs of *P. australis* using DPPH assay at concentration of 100 (µg/ml)

Antimicrobial activity

Table 5 shows that comparing *P. australis* ext. to AgNBs ext. form has a considerable influence on antibacterial activity, with some variation depending on the strain type. In comparison to native extracts, AgNBs may inhibit *Pseudomonas aeruginosa* (19 mm) and *Candida albicans* (22 mm). This result could be attributed to an increase in

AgNBs surface area. In instances of *Staphylococcus aureus*, *Bacillus cereus*, and *Escherichia coli*, the findings of AgNBs and, *P. australis* ext. differ dramatically. This indicates that AgNBs increase the extract's antibacterial action. Because nanosilver has a large specific surface area, it effectively interacts with bacterial RNA and severely limits their growth (Fig. 6) [37, 38].

Table 5: Antimicrobial activity expressed as inhibition diameter zones in millimeters (mm) of chemical compounds against the pathological strains based on well diffusion assay

Samples	Total extract	Nano extract	References
Test bacteria			CN MIZ
<i>Pseudomonas Aeruginosa</i>	15.0	19.0	15.0 -
<i>Bacillus cereus</i>	11.0	20.0	13.0 -
<i>Escherichia coli</i>	15.0	20.0	17.0 -
<i>Staphylococcus</i>	13.0	20.0	13.0 -
<i>Candida albicans</i>	20.0	22.0	- 11.0



Escherichia coli *Pseudomonas aeruginosa* *Candida albicans*



Bacillus cereus *Staphylococcus aureus*

Fig. 6 Inhibition zone diameter (millimeter) of the samples

4. Conclusion

The phytochemical studies of *Phragmites australis* using spectrometric techniques and LC–ESI–MS led to the isolation and identification of 22 natural flavonoid compounds. *P. australis* ethanolic extract has high free radical scavenging activity than its nano extract so it considered being natural free radical scavenging agents. Both *P. australis* ethanolic extract and its nano had a modest to no cytotoxic effect on the cancer cells tested A-431 (skin cancer), PC3 (prostate cell line), HCT-116 (colon cell line), and BJ-1 (normal skin fibroblast). As well as the antimicrobial results for both extracts showed a significant influence with some fluctuation depending on the strain type.

5. Conflicts of interest

There are no conflicts to declare

6. References

1-Christenhusz, M. J. M. and Byng, J. W., The number of known plants species in the world and its annual increase. *Phytotaxa*, 261 (3) 201–217, 2016.

- 2-Harborne, J. B., and Williams C. A., Flavonoid patterns in leaves of the Gramineae. *Biochem Syst. Ecol.* 4, 267–280, 1976.
- 3-Liqian, Z., Dong, Z., Chen Y., Xiuyan, D., Yu S., Yuting J., and Guoqiang Z., Anti-Inflammatory and antiviral effects of water-soluble crude extract from *Phragmites australis* in vitro. *Pak. J. Pharm. Sci.*, 30 (4) 1357-1362, 2017
- 4- Chen, S., Ju, M., Luo, Y., Chen, Z., Zhao, C., Zhou, Y., and Fu, J. Hepatoprotective and antioxidant activities of the aqueous extract from the rhizome of *Phragmites australis*. *Zeitschrift für Naturforschung C.*, 68, 439-444, 2013.
- 5- Sim, M.O., Ham, J.R., Lee, M. K., Young leaves of reed (*Phragmites communis*) suppress melanogenesis and oxidative stress in B16F10 melanoma cells. *Biomed. Pharmacother.*, 93, 165-171, 2017.
- 6- Zhu, L., Zhang, D., Yuan, C., Ding, X., Shang, Y., Jiang, Y., Zhu, G. Anti-Inflammatory and antiviral effects of water-soluble crude extract from *Phragmites australis* in vitro *Pak. J. Pharm. Sci.*, 30(4):1357-1362 (2017)
- 7- Wu Q. H., Treatment of liver disease by rhizome of reed. *Jilin Trad. Chin. Med.* 3, 35 -35, 1986.
- 8- Gao, H. X., Ding, A. W., Tang Y. P., Zhang X., and Duan J. A. Chemical constituents from the rhizomes of *Phragmites australis*, *Chin. J. Natl. Med.* 7, 196 -199, 2009.
- 9 - SATCM (State Administration of Traditional Chinese Medicine) *Zhonghuabencao*. Shanghai Sci-ence and Technology Press, Shanghai, China, 8, 390 – 393, 1999.
- 10- Zayed, M., Eisa, W., Abdel-Moneam, Y., El-kousy, S., Atia, A., Ziziphus spina-christi based bio-synthesis of Ag nanoparticles. *Journal of Industrial and Engineering Chemistry*, 23, 50–56, 2015.
- 11- Sun, T., Tang, J. and Powers, J.R., Effect of pectolytic enzyme preparations on the phenolic composition and antioxidant activity of asparagus juice. *Journal of Agricultural and Food Chemistry*, 53(1), 42-48, 2005.
- 12-Shinji M, Yuichi Y, Mikari E, Haruhiko M, Akira M, Motohiro T, Takuma S, Antitumor activity of a novel orally effective nucleoside, 1-(2-deoxy-2-fluoro-4-thio-β-D-arabinofuranosyl) cytosine, *Cancer letters*, 129 (1), 103-110, 1998.
- 13-Barry, A. L., Procedure for testing antimicrobial agent in agar media. In V. Lorian(ed) *Antibiotica in laboratory medicines*. Willims and Wilkins Co. Baltimore. 23(1), 1-23, 1980.
- 14-Frey, F.M and Rayan, M., Antibacterial activity of traditional medicinal plants used by Haudenosaunee peoples of New York State, *BMC Complementary and Altrnative Medicine*. 64(10), (2010).
- 15- Hindler, J. A.; Howard, B. J. and Keiser, J.F., *Antimicrobial agents and Susceptibility testing. Clinical and pathogenic Microbiology*. Mosby-Year Book Inc., St. Louis, MO, USA (1994).
- 16- Fatma, S., Abd El -Aal, H. Sh., Mohammed, M. H. I., and Lotfy D., I., Chemical profiling of polyphenols in *Thunbergia alata* and in silico virtualscreening of their antiviral activities against COVID-19. *Azhar Int J Pharm Med Sci.* 1 (2), 94-100, 2021.
- 17- Zhuan-Hong, Li., Han Guo, Wen-Bin Xu, Juan Ge, Xin Li, MireguliAlimu, and Da-Jun He, Rapid Identification of Flavonoid Constituents Directly

- from PTP1B Inhibitive Extract of Raspberry (Rubusidaeus L.) Leaves by HPLC–ESI–QTOF–MS–MS. *J Chromatogr Sci.*, 54(5), 805–810, 2016.
- 18- Rita, M., Micaela, M. S., Maria, C. Oliveira., Maria, J. M., Characterization of weld (Reseda luteola L.) and spurge flax (Daphne gnidium L.) by high-performance liquid chromatography–diode array detection–massspectrometry in Arraiolos historical textiles. *Journal of Chromatography*, 1216, 1395–1402, 2009.
- 18- Venkatalakshmi, P., Vadivel, V., Brindha, P., Identification of flavonoids in different parts of minaliacatappa L. Using LC-ESI-MS/MS and investigation of their anticancer effect in EAC cell line model. *Pharm.Sci.and Res*, 8, 176–183, 2016.
- 19- Fatma, S., Abd El -Aal, H. Sh., Mohammed, M. H. I., and Lotfy D., I., Chemical profiling of polyphenols in Thunbergialaata and in silico virtualscreening of their antiviral activities against COVID-19. *Azhar Int J Pharm Med Sci.* 1 (2), 94-100, 2021.
- 20- Zeliou, K.; Kouli, E.-M.; Papaioannou, C.; Koulakiotis, N.S.; Iatrou, G.; Tsarbopoulos, A.; Papisotiropoulos, V.; Lamari, F.N. Metabolomic fingerprinting and genetic discrimination of four Hypericum taxa from Greece. *Phytochemistry*, 174, 112290, 2020.
- 21- Jeevan, K., P., Kenneth, J., Marion, K., Landon, W., Michelle, S-J, Connie, W., Profiling and Quantification of Isoflavonoids in Kudzu Dietary Supplements by HPLC and ELSI-TMS. *J. Agric. Food Chem.*, 51(15): 4213-4218, 2003.
- 23-Al Sayed, E., Martiskainen, O., Sinkkonen, J., Pihiaja, K., Ayoub, N., Singab, A. E., et al., Chemical composition and bioactivity of Pleiogyniumtimorense (Anacardiaceae). *Natural Product Communications*, 5, 545–550, 2010.
- 24- Wu, S. J., Sun, A. L., Liu, R.M., *J Chro-matogr A* 1066, 243–247, 2005.
- 25- Gao, Q.; Ma, R.; Chen, L.; Shi, S.; Cai, P.; Zhang, S.; Xiang, H. Antioxidant profiling of vine tea (Ampelopsis grossedentata): Off-line coupling heart-cutting HSCCC with HPLC–DAD–QTOF–MS/MS. *Food Chem.* 225, 55–61, 2017.
- 26-Rita M, Micaela M. S, Maria C. O, Maria J. M, Characterization of weld (Reseda luteola L.) and spurge flax (Daphne gnidium L.) by high-performance liquid chromatography–diode array detection–mass spectrometry in Arraiolos historical textiles. *Journal of Chromatography*, 1216 1395–1402, 2009.
- 27- Wu, B.; Song, H.-P.; Zhou, X.; Liu, X.G.; Gao, W.; Dong, X.; Li, H.-J.; Li, P.; Yang, H. Screening of minor bioactive compounds from herbal medicines by in silico docking and the trace peak exposure methods. *J. Chromatogr. A.* 1436, 91–99, 2016.
- 28-Kim, M.Y., Chung, I. M., Choi, D. C., and Park, H. J. Quantitative analysis of fustin and sulfuretin in the inner and outer heartwoods and stem bark of Rhusvernificflua. *Natural Product Sciences*, 15, 208–212, 2009.
- 29 -Rivero, P., Goicoechea J, Urrutia A, Arregui F. Effect of both protective and reducing agents in the synthesis of multicolor silver nanoparticles. *Nanoscale Research Letters*, 8, 101-109, (2013).
- 30- Sastry, M., Mayya, K. S., and Bandyopadhyay, K., pH Dependent changes in the optical properties of carboxylic acid derivatized silver colloidal particles. *Colloids Surf. A: Physicochem. and Engi. Aspects* 127, 221–228, 1997.
- 31- Rai, M., Yadav, A., Plants as potential synthesiser of precious metal nanoparticles. progress and prospects. *IET Nanobiotechnol*, 7, 117-124, 2013.
- 32-Thakkar, K.N., Mhatre, S.S., Parikh, R.Y., Biological synthesis of metallic nanoparticles. *Nanomedicine*, 6, 257-262, 2010.
- 33-Samfira, I., Rodino, S., Petrache, P., Cristina, R.T., Butu, M., Butnariu, M., Characterization And Identity Confirmation Of Essential Oils By Mid Infrared Absorption Spectrophotometry. *DIGEST journal of nanomaterials and biostructures*. 10 (2), 557-565, 2015.
- 34- Al-Snafi AE. The constituents and biological effects of Arundo donax - A review. *International Journal of Phytopharmacy Research*, 6 (1): 34-40, 2015.
- 35- Park, J., Gim, S. Y. , Jeon, J.Y. , Kim, M. J. , Choi, H.K, and Lee, J. Chemical profiles and antioxidant properties of roasted rice hull extracts in bulk oil and oil-in-water emulsion. *Food Chemistry*, 272, 242–250, 2019.
- 36- Parker, T. D., Adams, D., Zhou, K., Harris, M., & Yu, L. Fatty acid composition and oxidative stability of cold-pressed edible seed oils. *Journal of Food Science*, 68(4), 1240–1243, 2003.
- 37- Leporatti ML and Impieri M. Ethnobotanical notes about some uses of medicinal plants in Alto TirrenoCosentino area (Calabria, Southern Italy). *Journal of Ethnobiology and Ethnomedicine*, 3, 34-39, 2009.
- 38- Wang L, Hu C, and Shao L. The antimicrobial activity of nanoparticles: present situation and prospects for the future. *Int J Nanomedicine*, 12: 1227–1249, 2017.